

# Probing Pb+Pb collisions at $\sqrt{S_{NN}} = 2760$ GeV with spectators

Vipul Bairathi,<sup>1,\*</sup> Sandeep Chatterjee,<sup>2,†</sup> Md. Rihan Haque,<sup>1,‡</sup> and Bedangadas Mohanty<sup>1,§</sup>

<sup>1</sup>*School of Physical Sciences, National Institute of Science Education and Research, Jatni, 752050, India*

<sup>2</sup>*Theoretical Physics Division, Variable Energy Cyclotron Centre, 1/AF Bidhannagar, Kolkata, 700064, India*

## Abstract

There is event by event geometric as well as quantum fluctuations in the initial condition of heavy-ion collisions. The standard technique of analysing heavy-ion collisions in bins of centrality obtained from final state multiplicity averages out the various initial configurations and thus restricts the study to only a limited range of initial conditions. In this paper, we propose an additional binning in terms of total spectator neutrons in an event. This offers us a key control parameter to probe events with broader range of initial conditions providing us an opportunity to peep into events with rarer initial conditions which otherwise get masked when analysed by centrality binning alone. We find that the inclusion of spectator binning allows one to vary  $\varepsilon_2$  and  $\varepsilon_3$  independently. We observe that the standard scaling relation between  $v_2/\varepsilon_2$  and  $\frac{1}{S} \frac{dN_{ch}}{dn}$  exhibited by centrality bins is broken by the spectator neutron bins. However, the acoustic scaling relation between  $\ln(v_n/\varepsilon_n)$  and transverse system size holds for both centrality as well as spectator bins for central to mid-central collisions. The introduction of the spectator binning allows us to tune over a wide range viscosity driven effects for events with varying initial states but similar final state multiplicity.

arXiv:1508.02338v1 [nucl-th] 10 Aug 2015

---

\* vipul.bairathi@niser.ac.in

† sandeepc@vecc.gov.in

‡ rihan.h@niser.ac.in

§ bedanga@niser.ac.in

## I. INTRODUCTION

Of all the stages in a heavy-ion collision (HIC), the initial stage is the least understood. However, in order to perform a sensitive test of the theoretical framework, e.g. relativistic viscous hydrodynamics, that correctly describes the evolution of the strongly interacting matter produced in HIC experiments and thereof allows unambiguous extraction of the medium properties, e.g. values of the transport coefficients, require a precise knowledge of the initial state (IS). It has been shown that depending on the choice of the initial condition that one chooses to evolve the relativistic hydrodynamic equations, the value of the extracted shear viscosity to entropy density ratio at the RHIC 200 GeV can vary by a factor of 2 [1–6].

The nuclei used in HIC experiments are extended objects. This results in event by event (E/E) geometrical fluctuations in addition to the intrinsic quantum fluctuations of the nuclear wave function. The geometry of the nucleus ensures that various characteristics of the IS in HICs like the number of wounded nucleons  $N_{\text{part}}$ , number of binary collisions  $N_{\text{coll}}$ , shape of the overlap region, say the ellipticity  $\varepsilon_2$ , are all correlated with the impact parameter  $b$ . However, none of the above IS collision attributes are directly observed in experiments. This makes the job to constrain the IS very challenging. The standard method uses the final state (FS) charged particle multiplicity to characterize the events into different centrality classes corresponding to different ISs. However, the geometric and quantum E/E fluctuations in the IS result in appreciable variation of  $b$ ,  $N_{\text{part}}$ ,  $N_{\text{coll}}$ ,  $\varepsilon_2$  etc., even within the same centrality bin. Thus, a lack of proper knowledge of the IS is a major hindrance towards carrying out precise comparisons between theory and experiments. In this work, we focus on the spectators (those nucleons which do not participate in the collision) and show that it is possible to extract vital information of the IS by analysing them. The significant role played by spectator asymmetry in the various experimental observables and the possibility of selecting special initial configurations in HIC using deformed U nuclei has been pointed out recently [7, 8]. In a study based on Monte Carlo Glauber model simulations it was suggested that spectator asymmetry could be used to trigger specific collision configurations called Body-Tip with sufficient magnetic field and much lower ellipticity which can lead to the disentanglement of chiral magnetic effect from its dominant background anisotropic flow in  $U + U$  collisions [7]. In Ref. [8] it was demonstrated based on A Multi Phase Transport (AMPT) model simulations that spectator asymmetry could be utilised to identify Body-Tip collision configurations in  $U + U$  with large forward-backward asymmetry in particle production as well as considerably smaller elliptic flow,  $v_2$ . In this work, we look into the possibility of probing HICs of non-deformed nuclei using spectators. We will in particular focus on  $Pb + Pb$  collisions at  $\sqrt{s_{\text{NN}}} = 2760$  GeV. A recent study has pointed out the correlation between forward-backward asymmetry in particle production and spectator asymmetry in  $Pb + Pb$  collisions at  $\sqrt{s_{\text{NN}}} = 2760$  GeV [9].

We have constructed an IS observable, namely the total spectator neutron ( $L+R$ ), which is the sum of the left going (L) and right going (R) spectator neutrons that are detected by the zero degree calorimeters (ZDC). In the absence of the IS fluctuations,  $L + R$  and  $b$  would have a one to one correspondence. Both quantities are zero for full overlap collisions and increase for peripheral collisions. The advantage of  $L + R$  is that it is an observable measured in experiments while  $b$  is never measured. We demonstrate that by performing a further binning over  $L + R$  in addition to the standard centrality binning, it is possible to probe the fireball with novel IS conditions as compared to centrality binning alone. This allows us to perform a more accurate comparison between model predictions and data, thus enabling a more precise modelling and comprehensive understanding of the response of the strongly interacting matter to the IS conditions created in HIC experiments. The outline of the paper is as follows: in the next section II we discuss the details of the AMPT model and our simulation as well as our proposed methodology to bin events. In Sec. III, we show the main results obtained with this new binning procedure and finally summarise in Sec. IV.

## II. MODEL

We have simulated  $Pb + Pb$  collisions at  $\sqrt{s_{\text{NN}}} = 2760$  GeV using A Multi Phase Transport (AMPT) [10, 11] model in the Default version. The AMPT model uses the same initial conditions as HIJING [12]. Zhangs parton cascade follows to take into account partonic interactions [13] which finally recombine with their parent strings that fragment into hadrons within the Lund String Fragmentation model [14]. There is a final stage hadronic afterburner before the hadrons freezeout. In this study we have analysed  $\sim 2 \times 10^6$  events.

The standard practice is to first categorize events into different centrality classes according to charged particle multiplicity. This is shown in Fig. 1 (a). The different centrality classes are shown in alternate white and grey bands. Here we propose to do a second round of binning with the observable  $L + R$  within each centrality bin. The  $L + R$  binning is illustrated in Fig. 1 (b) where the  $L + R$  distribution is shown for (10 – 15)% centrality. The  $L + R$

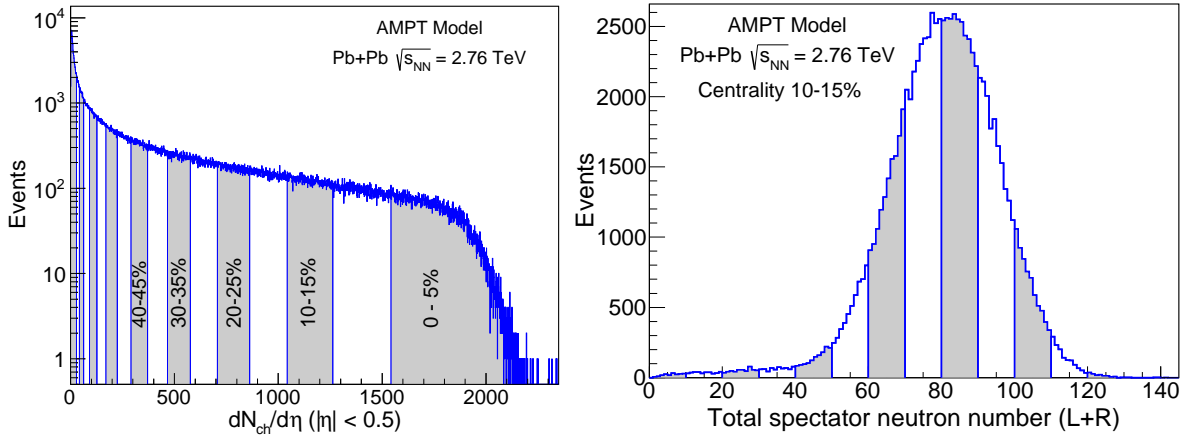


FIG. 1. (Color online) Left: The multiplicity distribution for min bias Pb-Pb events at  $\sqrt{s_{NN}} = 2760$  GeV. In alternate white and grey bands, different centrality bins are also shown. Right: The total spectator neutron number  $L + R$  distribution for the (10 – 15) % centrality. The different  $L + R$  bins are also shown.

distribution shows a prominent peak around 85-95 and falls off rapidly on either side - the number of events drop by a factor of 5 as  $L + R$  shifts by  $\sim 20$ . Thus when the analysis is performed based on centrality binning alone, we mainly study properties of the events with total spectator neutrons around 85-95. Here with the introduction of the  $L + R$  binning, we can investigate properties of the rare events with fewer or higher values of  $L + R$  compared to the centrality mean value. This is the basic reason why additional  $L + R$  binning on top of the centrality binning allows us to study new IS conditions in HICs.

### III. RESULTS AND DISCUSSION

We will now present the results of our analysis based on the spectator binning on top of the multiplicity binning. We show the results from centrality binning alone by the open triangles joined by a dotted line. Here we propose to further bin each such centrality bin into different  $L + R$  spectator bins as well. These are shown by the colored symbols, each color representing a centrality bin.

Due to E/E fluctuation of the participant positions, the principal axes of inertia of the participant (P) nucleons is shifted as well as tilted with respect to those of the nucleus-nucleus (N) system [15]. Hence, we first perform the necessary translation,

$$x' = x_N - \langle x_N \rangle, \quad (1)$$

$$y' = y_N - \langle y_N \rangle, \quad (2)$$

where  $(x_N, y_N)$  denote the nucleon coordinates in the N coordinate system, and further rotate the primed coordinate system by the second order participant plane angle  $\Psi_2^{PP}$ , so as to coincide with the P coordinate system.  $\Psi_2^{PP}$  is obtained as follows,

$$\varepsilon_n e^{i\Psi_n^{PP}} = \frac{\sum_i r_i^n e^{in\phi'_i}}{\sum_i r_i^n}, \quad (3)$$

where  $(r'_i, \phi'_i)$  is the new 2-D polar coordinate of the  $i$ th participant in the primed coordinate system.  $\Psi_2^{PP}$  is obtained for  $n = 2$ . The initial spatial geometry of the overlap region is encoded in the eccentricities  $\varepsilon_n$  defined in Eq. 3 of which  $\varepsilon_2$  and  $\varepsilon_3$  will be discussed in this work.

We will first analyse the distribution of the participants in the plane transverse to the collision axis, which we call the collision plane. In Figs. 2 (a) and 2 (b) we have plotted the bin average of the standard deviation in the  $x_P$  ( $\sigma_x = \sqrt{\langle x_P^2 \rangle - \langle x_P \rangle^2}$ ) and  $y_P$  ( $\sigma_y = \sqrt{\langle y_P^2 \rangle - \langle y_P \rangle^2}$ ) coordinates of the participants measured with respect to the P coordinate system.  $\sigma_x$  and  $\sigma_y$  gives us an idea of the initial size of the fireball on the collision plane at the time of

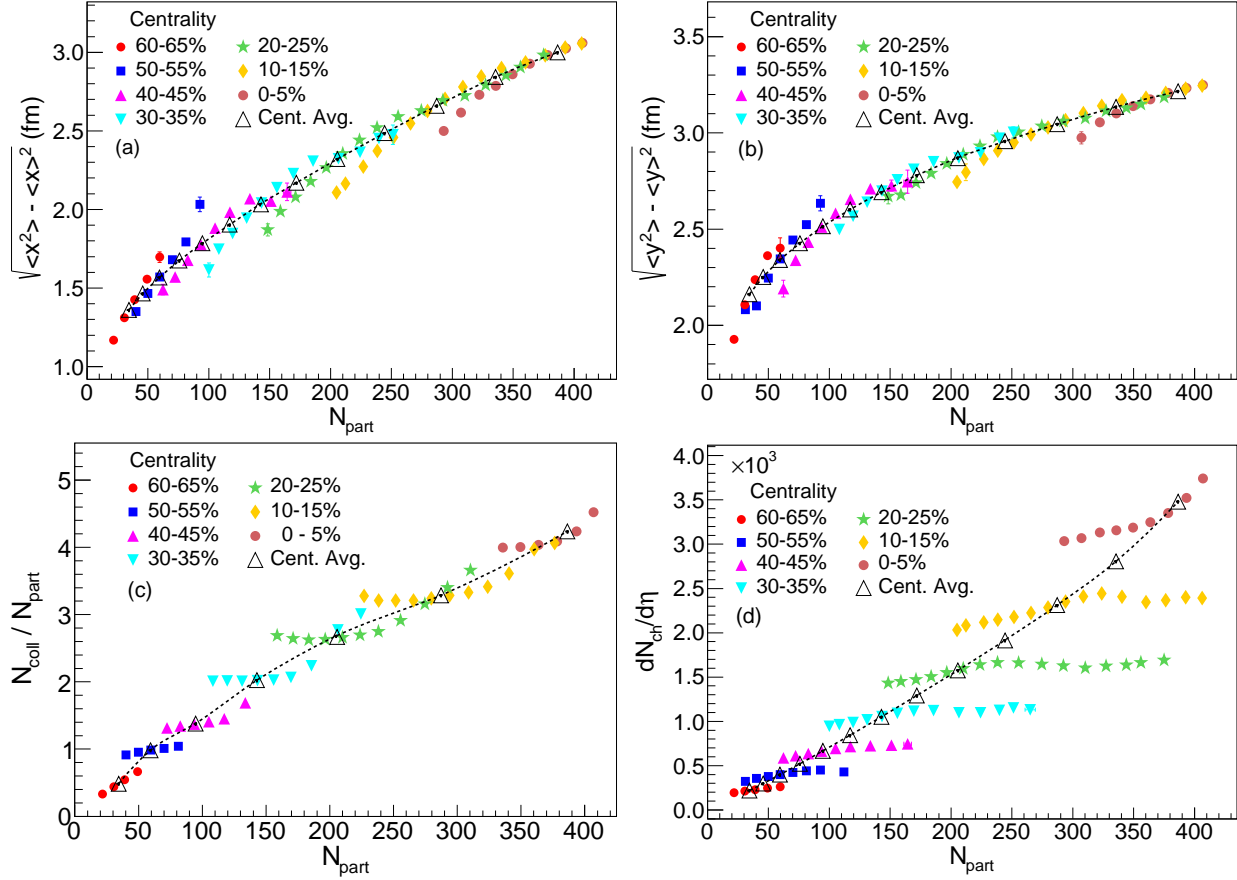


FIG. 2. (Color online) Different qualitative dependence of  $\sigma_x$ ,  $\sigma_y$ ,  $N_{\text{coll}}$  and  $dN_{ch}/d\eta$  on  $N_{\text{part}}$  with centrality bins and  $L + R$  bins.

collision. The curves for  $\sigma_x$  and  $\sigma_y$  vs  $N_{\text{part}}$  show different correlations along centrality and  $L + R$  bins. They both decrease more rapidly along  $L + R$  bins than along centrality bins. This brings us to Fig. 2 (c) where the number of binary collisions,  $N_{\text{coll}}$  is shown normalised to  $N_{\text{part}}$ , the number of participants. Within a geometry based approach of particle production and initial conditions in HICs, e.g. the two component Glauber model,  $N_{\text{part}}$  and  $N_{\text{coll}}$  are the two most essential ingredients that determine the IS as well as the FS multiplicity [16–18]. A collision between two nucleons (one from each of the colliding nucleus A and B) with coordinates  $(x_A, y_A)$  and  $(x_B, y_B)$  on the collision plane occurs if they satisfy the following simple geometrical criteria

$$(x_A - x_B)^2 + (y_A - y_B)^2 \leq \frac{\sigma_{NN}}{\pi} \quad (4)$$

where  $\sigma_{NN}$  is the nucleon-nucleon cross section.  $N_{\text{part}}$  is the sum of all the nucleons that satisfy Eq. 4.  $N_{\text{coll}}$ , on the other hand, is the sum of all such possible binary collisions between the participants. The distribution of the participants on the collision plane determine the IS eccentricities given by Eq. 3. As shown in Fig. 2 (c), the  $L + R$  bins of a higher centrality bin mostly have larger value of  $N_{\text{coll}}$  compared to a lower centrality bin. This is so because as seen in Figs. 2 (a) and (b), bins with same  $N_{\text{part}}$  but higher centrality occupy a smaller area on the collision plane as implied by smaller values of  $\sigma_x$  and  $\sigma_y$ . This means the participants are more lined up along the beam axis than perpendicular to it, hence having a higher value for  $N_{\text{coll}}$  and smaller  $\sigma_x$  and  $\sigma_y$ . Finally in Fig. 2 (d) we have plotted  $dN_{ch}/d\eta$  vs  $N_{\text{part}}$ . Clearly, the correlations along centrality bins is different from that along the  $L + R$  bins. In a given centrality bin as  $L + R$  increases,  $N_{\text{part}}$  decreases. However,  $dN_{ch}/d\eta$  almost remains constant which in turn implies constancy of the initial energy deposited even though  $N_{\text{part}}$  decreases. This suggests that in a given centrality, as we go towards bins with larger  $L + R$ , the energy deposit pattern changes- one expects to find larger energy gradients and more number of energy hot spots (as the same energy is deposited over a smaller transverse area by lesser  $N_{\text{part}}$ ).

This should result in very different viscous effects as one scans over bins with varying  $L + R$  at a given centrality which will be best borne out by observables on anisotropic flow.

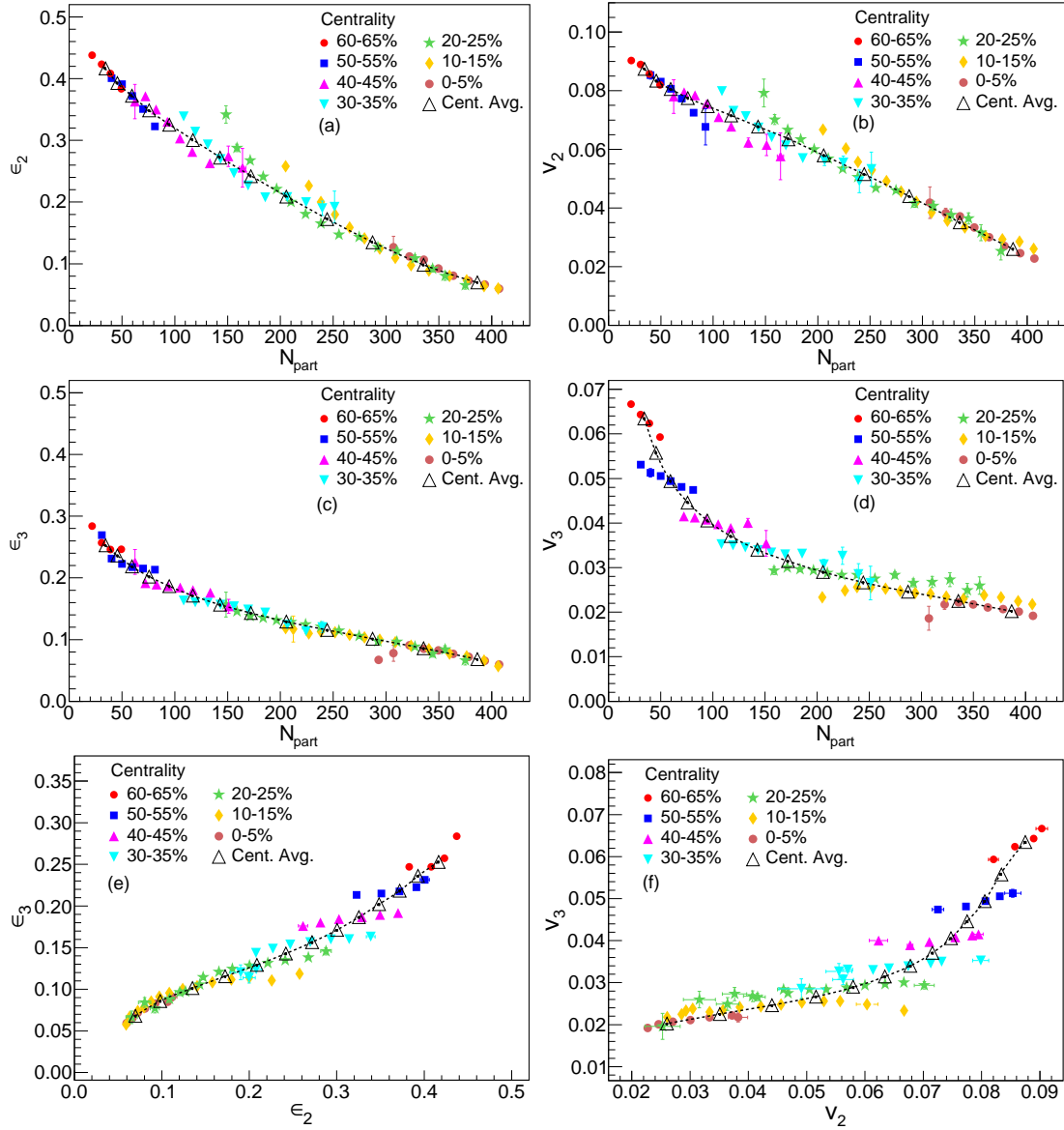


FIG. 3. (Color online) Different qualitative dependence of  $\epsilon_2$ ,  $\epsilon_3$ ,  $v_2$  and  $v_3$  on  $N_{\text{part}}$  with centrality bins and  $L + R$  bins are shown. We also show the correlation between  $\epsilon_2$  and  $\epsilon_3$  as well as between  $v_2$  and  $v_3$  with centrality and  $L + R$  bins.

The collective hydrodynamic response converts the IS spatial anisotropy of the fireball as reflected by  $\epsilon_n$  into the

FS azimuthal anisotropy of the produced charged particle characterised by the flow observables  $(v_n, \Psi_n^{EP})$ ,

$$\frac{dN}{d\phi} \propto 1 + 2 \sum_{n=1}^{\infty} v_n \cos(n(\phi - \Psi_n^{EP})) = 1 + 2 \sum_{n=1}^{\infty} (v_{n,x} \cos(n\phi) + v_{n,y} \sin(n\phi)), \quad (5)$$

$$Q_{n,x} = \sum_i^M \cos(n\phi_i), \quad Q_{n,y} = \sum_i^M \sin(n\phi_i), \quad (6)$$

$$v_{n,x} = \frac{1}{M} Q_{n,x}, \quad v_{n,y} = \frac{1}{M} Q_{n,y}, \quad v_n = \sqrt{v_{n,x}^2 + v_{n,y}^2} \quad (7)$$

Here  $\phi_i$  is the azimuthal angle of the  $i$ th particle,  $M$  is the total number of particles and  $\Psi_n^{EP}$  is the event plane angle, measured using the produced particles [19]. There have been attempts to study the influence of the initial event shape on the ensuing fireball dynamics and hence on various FS observables [20, 21]. We now focus our attention on the event shape- how  $L + R$  binning introduces a control parameter to tune the IS geometry.

As seen in Fig. 3,  $\varepsilon_2$  and  $\varepsilon_3$  show almost similar variation along centrality and spectator bins for central events. For mid-central to peripheral bins, starting from (20 – 25) % centrality bin, the correlation between  $\varepsilon_2$  and  $N_{\text{part}}$  along spectator bins is slightly steeper compared to that along centrality bins. On the other hand,  $\varepsilon_3$  correlation with  $N_{\text{part}}$  is gentler along  $L + R$  bins. This difference in variation of  $\varepsilon_2$  and  $\varepsilon_3$  along  $L + R$  vs centrality bins becomes more transparent in the FS flow observables,  $v_2$  and  $v_3$  as shown in Figs. 3 (b) and (d). This also gives rise to the  $\varepsilon_2 - \varepsilon_3$  and  $v_2 - v_3$  correlation plots as shown in Figs. 3 (e) and (f). For (20 – 25) % and more peripheral bins, there is much smaller correlation along  $L + R$  bins as compared to that along centrality bins, e.g. in case of the (20 – 25) % centrality bin while  $v_3$  changes by only 10% for different  $L + R$  bins,  $v_2$  varies by around 130%. This will allow us to disentangle the effects of  $v_2$  from  $v_3$  on other observables like higher flow harmonics etc. Thus, a combined binning in terms of centrality and  $L + R$  allows us to disentangle the contribution of different IS characteristics on the FS observables. Here we have discussed two such cases, (a)  $N_{\text{part}}$  and  $N_{\text{coll}}$  and their contribution towards FS  $dN_{ch}/d\eta$  and (b)  $\varepsilon_2$  and  $\varepsilon_3$  and their contribution towards  $v_2$  and  $v_3$  respectively. Thus studies with  $L + R$  bins can complement ongoing studies with  $q_2$  bins which also aim at studying the influence of the event shape on various FS observables [20, 21] where  $q_2$  is obtained from the the second harmonic flow vector  $Q_2$  [19, 20]

$$Q_2 = \sqrt{Q_{2,x}^2 + Q_{2,y}^2}, \quad q_2 = \frac{1}{\sqrt{M}} Q_2 \quad (8)$$

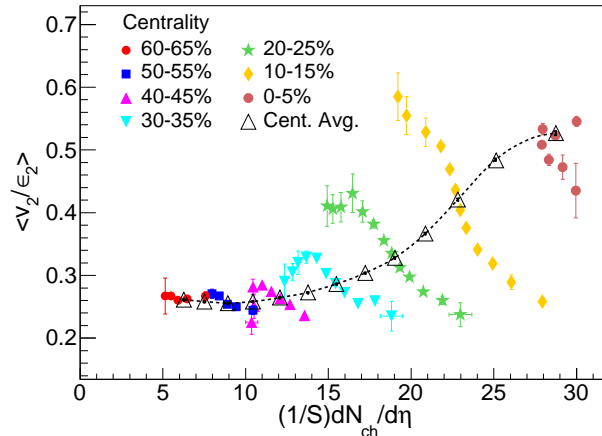


FIG. 4. (Color online)  $v_2/\varepsilon_2$  vs  $(1/S) dN_{ch}/d\eta$  for different centrality and  $L + R$  bins. The  $L + R$  bins break the scaling relation between  $v_2/\varepsilon_2$  and  $(1/S) dN_{ch}/d\eta$  that is exhibited by centrality bins.

Ideal fluid hydrodynamics is scale invariant and as a result the final value of the ratio  $(v_2/\varepsilon_2)$  attained is independent of the system size [22]. Viscous corrections in a non-ideal fluid arising due to incomplete thermalization introduce system size dependence and tend to reduce this ratio. The ratio of the microscopic mean free path  $\lambda$  to the typical macroscopic system size  $\Lambda$ ,  $\lambda/\Lambda$  is called the Knudsen number  $K$ .  $K^{-1}$  is expected to be a good measure of the

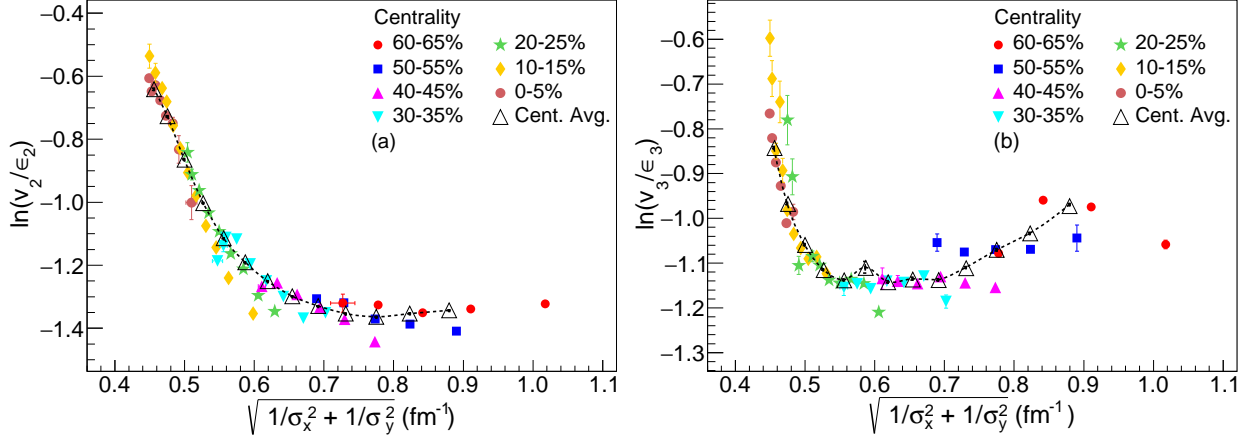


FIG. 5. (Color online) Acoustic scaling of the hydrodynamic response  $\ln(v_n/\varepsilon_n)$  vs  $1/\Lambda_T$  with  $n = 2$  (left) and  $n = 3$  (right) for different centrality and  $L + R$  bins.

thermalization achieved [1, 22]. Since  $v_2$  develops over some time during which the fireball rapidly expands it is not exactly clear what should be the value of  $\lambda$  and  $\Lambda$  to be used to determine the degree of thermalization. In earlier studies, it has been suggested that  $v_2$  dominantly develops in the early stage of the fireball evolution. Therefore  $K^{-1}$  estimated at time  $\tau \sim \Lambda_T/c_s$  at the onset of transverse expansion of the fireball, should be used as a measure of thermalization [1, 22]. Here  $\Lambda_T$  is the transverse size of the fireball on the collision plane and  $c_s$  is the speed of sound. It was further argued that  $K^{-1}$  at  $\Lambda_T/c_s$  approximately scales with  $(1/S) dN_{ch}/d\eta$  where  $S$  is the initial transverse area on the collision plane. Similar scaling relation between  $v_2/\varepsilon_2$  and  $(1/S) dN_{ch}/d\eta$  is also expected in the low density regime [23–25]. Previous analysis of experimental data with centrality binning have indeed found very good scaling relation between  $v_2/\varepsilon_2$  vs  $(1/S) dN_{ch}/d\eta$  for different systems like Cu+Cu and Au+Au [1, 4]. The detailed mechanism of energy deposition in the initial stages of a HIC event which ultimately leads to particle production is yet to be understood completely. With centrality as the only tuning parameter to separate different initial conditions, it is difficult to discriminate between predictions from models with different mechanisms of particle production. Now, with the introduction of  $L + R$  bins, we are able to pin down the initial conditions more precisely. In Fig. 4 we have plotted the ratio  $v_2/\varepsilon_2$  vs  $(1/S) dN_{ch}/d\eta$  with centrality and  $L + R$  bins. The centrality averaged points exhibit the usual trend of an initial fast rise and final saturation of the ratio  $v_2/\varepsilon_2$  with  $(1/S) dN_{ch}/d\eta$ . However, the  $L + R$  bins in each centrality show the opposite behaviour and breaks the usual scaling relation. In a given centrality bin, with rise in  $L + R$ , the transverse overlap area  $S$  sharply falls while  $dN_{ch}/d\eta$  is almost constant. Thus  $(1/S) dN_{ch}/d\eta$  which acts like a proxy for  $K^{-1}$  increases with  $L + R$  although the hydrodynamic response  $v_2/\varepsilon_2$  falls sharply. As mentioned earlier, we expect more (less) hot spots and gradients in the initial energy profile of events with larger (smaller)  $L + R$  leading to more (less) viscous correction. This ultimately leads to inefficient conversion of the initial  $\varepsilon_n$  to the final  $v_n$  in events with larger  $L + R$  as compared to those with smaller  $L + R$ .

The ratio  $v_n/\varepsilon_n$  is also expected to exhibit acoustic scaling and receives viscous corrections that grow exponentially as  $n^2$  and  $1/\Lambda_T$  [26–29]

$$\ln\left(\frac{v_n}{\varepsilon_n}\right) \propto -\frac{4}{3} \frac{n^2 \eta}{\Lambda_T T s}, \quad (9)$$

with the typical initial transverse size of the system  $\Lambda_T$  given by  $1/\Lambda_T = \sqrt{1/\sigma_x^2 + 1/\sigma_y^2}$ . Such acoustic scaling was found in data across a wide range of beam energies and the shear viscosity to entropy density ratio,  $\eta/s$  was extracted from the slope of the plot,  $\ln\left(\frac{v_2}{\varepsilon_2}\right)$  vs  $1/\Lambda_T$  [27–29]. These studies were done with centrality binning alone. Here we perform a consistency check of such scaling laws using simulated data by including  $L + R$  bins in every centrality bin. In Figs. 5 (a) and (b) we have plotted  $\ln(v_2/\varepsilon_2)$  and  $\ln(v_3/\varepsilon_3)$  respectively vs  $1/\Lambda_T$ . We find simulated data collapse for (0–40)% centrality as well as their corresponding  $L + R$  bins. On a closer look, it seems that the slope parameter for bins of different  $L + R$  but a particular centrality is different from those of a different centrality. Thus, the introduction of the  $L + R$  bins enable a more refined extraction of  $\eta/s$  from data.

## IV. SUMMARY

We have demonstrated using the AMPT model the important role played by the spectators to determine the initial condition in heavy-ion collisions. The standard procedure involves binning events by their final state multiplicity. This however puts events with varying initial conditions into the same bin as long as they produce similar multiplicity. We demonstrate that by further binning events according to the total number of spectator neutrons, it is possible to separate events with different initial conditions which were earlier clubbed together in the same centrality bin. This new methodology provides an opportunity to study events with rare initial conditions. We found the variation of  $dN_{ch}/d\eta$  with  $N_{part}$  to be much different for  $L + R$  bins compared to usual centrality bins thus allowing us to study different energy deposition mechanism within the same centrality. We argued that in a given centrality bin, larger  $L + R$  bins have higher energy gradients and more number of energy hot spots as compared to smaller  $L + R$  bins which result in strong inhomogeneities in the initial conditions. This calls for larger viscosity driven effects and hence smaller  $v_2/\varepsilon_2$  for bins with higher  $L + R$ . This also results in the breaking of the scaling relation between  $v_2/\varepsilon_2$  and  $\frac{1}{s}dN_{ch}/d\eta$  by the  $L + R$  bins. On the other hand, the acoustic scaling relation between  $\ln(v_n/\varepsilon_n)$  and the initial system transverse size holds very well for both centrality as well as  $L + R$  bins. The results from this model study suggest that one might be able to extract a more accurate value of the  $\eta/s$  ratio with the introduction of the  $L + R$  bins.

## V. ACKNOWLEDGEMENT

SC acknowledges “Centre for Nuclear Theory” [PIC XII-R&D-VEC-5.02.0500], Variable Energy Cyclotron Centre, India for support. BM acknowledges financial support by the DAE-SRC and DST-Swarnjayanti projects.

- 
- [1] H.-J. Drescher, A. Dumitru, C. Gombeaud, and J.-Y. Ollitrault, Phys. Rev. **C 76**, 024905 (2007), arXiv:0704.3553 [nucl-th].
  - [2] P. Romatschke and U. Romatschke, Phys. Rev. Lett. **99**, 172301 (2007), arXiv:0706.1522 [nucl-th].
  - [3] M. Luzum and P. Romatschke, Phys. Rev. **C 78**, 034915 (2008), [Erratum: Phys. Rev. **C79**,039903(2009)], arXiv:0804.4015 [nucl-th].
  - [4] H. Song, S. A. Bass, U. Heinz, T. Hirano, and C. Shen, Phys. Rev. Lett. **106**, 192301 (2011), [Erratum: Phys. Rev. Lett. **109**,139904(2012)], arXiv:1011.2783 [nucl-th].
  - [5] V. Roy, A. K. Chaudhuri, and B. Mohanty, Phys. Rev. **C 86**, 014902 (2012), arXiv:1204.2347 [nucl-th].
  - [6] V. Roy, B. Mohanty, and A. K. Chaudhuri, J. Phys. **G 40**, 065103 (2013), arXiv:1210.1700 [nucl-th].
  - [7] S. Chatterjee and P. Tribedy, Phys. Rev. **C 92**, 011902 (2015), arXiv:1412.5103 [nucl-th].
  - [8] V. Bairathi, M. R. Haque, and B. Mohanty, Phys. Rev. **C 91**, 054903 (2015), arXiv:1504.04719 [nucl-ex].
  - [9] J. Jia, S. Radhakrishnan, and M. Zhou, (2015), arXiv:1506.03496 [nucl-th].
  - [10] Z.-w. Lin and C. Ko, Phys. Rev. **C 65**, 034904 (2002), arXiv:nucl-th/0108039 [nucl-th].
  - [11] Z.-W. Lin, C. M. Ko, B.-A. Li, B. Zhang, and S. Pal, Phys. Rev. **C 72**, 064901 (2005), arXiv:nucl-th/0411110 [nucl-th].
  - [12] X.-N. Wang and M. Gyulassy, Phys. Rev. **D 44**, 3501 (1991).
  - [13] B. Zhang, Comput. Phys. Commun. **109**, 193 (1998), arXiv:nucl-th/9709009 [nucl-th].
  - [14] B. Andersson, G. Gustafson, G. Ingelman, and T. Sjostrand, Phys. Rept. **97**, 31 (1983).
  - [15] R. S. Bhalerao and J.-Y. Ollitrault, Phys. Lett. **B 641**, 260 (2006), arXiv:nucl-th/0607009 [nucl-th].
  - [16] A. Bialas, M. Bleszynski, and W. Czyz, Nucl. Phys. **B 111**, 461 (1976).
  - [17] X.-N. Wang and M. Gyulassy, Phys. Rev. Lett. **86**, 3496 (2001), arXiv:nucl-th/0008014 [nucl-th].
  - [18] D. Kharzeev and M. Nardi, Phys. Lett. **B 507**, 121 (2001), arXiv:nucl-th/0012025 [nucl-th].
  - [19] A. M. Poskanzer and S. A. Voloshin, Phys. Rev. **C 58**, 1671 (1998), arXiv:nucl-ex/9805001 [nucl-ex].
  - [20] J. Schukraft, A. Timmins, and S. A. Voloshin, Phys. Lett. **B 719**, 394 (2013), arXiv:1208.4563 [nucl-ex].
  - [21] P. Huo, J. Jia, and S. Mohapatra, Phys. Rev. **C 90**, 024910 (2014), arXiv:1311.7091 [nucl-ex].
  - [22] R. S. Bhalerao, J.-P. Blaizot, N. Borghini, and J.-Y. Ollitrault, Phys. Lett. **B 627**, 49 (2005), arXiv:nucl-th/0508009 [nucl-th].
  - [23] H. Heiselberg and A.-M. Levy, Phys. Rev. **C 59**, 2716 (1999), arXiv:nucl-th/9812034 [nucl-th].
  - [24] S. A. Voloshin and A. M. Poskanzer, Phys. Lett. **B 474**, 27 (2000), arXiv:nucl-th/9906075 [nucl-th].
  - [25] P. F. Kolb, P. Huovinen, U. W. Heinz, and H. Heiselberg, Phys. Lett. **B 500**, 232 (2001), arXiv:hep-ph/0012137 [hep-ph].
  - [26] P. Staig and E. Shuryak, Phys. Rev. **C 84**, 034908 (2011), arXiv:1008.3139 [nucl-th].
  - [27] R. A. Lacey, A. Taranenko, N. N. Ajitanand, and J. M. Alexander, (2011), arXiv:1105.3782 [nucl-ex].

- [28] R. A. Lacey, Y. Gu, X. Gong, D. Reynolds, N. Ajitanand, et al., (2013), arXiv:1301.0165.
- [29] R. A. Lacey, A. Taranenko, J. Jia, D. Reynolds, N. Ajitanand, et al., Phys. Rev. Lett. **112**, 082302 (2014), arXiv:1305.3341 [nucl-ex].